

Is pre-stress important for simulating lung pneumothorax?

P. Alvarez, M. Chabanas and Y. Payan

Univ. Grenoble Alpes, CNRS, Grenoble INP, TIMC, Grenoble, France

1. Introduction

Biomechanical modeling of soft tissue has leveraged the development of computer systems to assist the planning and guidance of many clinical interventions (Payan 2012). However, the use of these systems in current clinical practice remains limited, since their accuracy still does not comply with the strict clinical requirements. Among the many factors having an impact on such accuracy, one that is often disregarded is the effect of pre-stress.

Typically, the geometry used for biomechanical simulations is computed from medical images, in which soft-tissue is already subject to various loads. In the case of the lung, for instance, an image at the end-of-exhalation will provide a lung geometry subject to the effects of gravity and negative intrapleural pressure. Assuming that the lung geometry extracted from this end-of-exhalation image is stress-free may compromise the accuracy of lung simulations.

In this paper, we investigate the effect of accounting for pre-stress in the simulation of lung pneumothorax (lung deflation), which is a phenomenon occurring during thoracic surgery. Improved modeling of pneumothorax may help to develop more accurate surgical guidance systems for thoracic surgery.

2. Methods

2.1. Biomechanical lung model

Following our previous work on the biomechanical simulation of lung pneumothorax (Alvarez et al. 2021), in this work, we used a poroelastic biomechanical model of the lung. This model is more realistic than elasticity models as it allows macroscopic modeling of air-parenchyma interactions.

The geometry of a left lung was segmented in the preoperative CT of a lung-cancer patient treated at Rennes University Hospital (ethics committee authorization No. 2016-A01353-48 35RC16 9838). From this segmentation, a Finite Element (FE) mesh of linear tetrahedral elements was generated using Altair Hypermesh, as well as linear-triangle contact surfaces for the lung and the thoracic wall.

Table 1. Material properties for the poroelastic biomechanical lung model.

Parameter	Value	Source
C_1	115 Pa	Fit from reference lung P-V curves
C_2	95 Pa	(Jafari et al. 2021)
C_3	210 Pa	(Jafari et al. 2021)
ν	0.4	(Jafari et al. 2021)
ϕ	0.9	Fit from reference lung volume values

C_1 , C_2 , and C_3 are material constants for the Yeoh model; ν is the Poisson's ratio; and ϕ is the porosity of the porous medium.

We used ANSYS Mechanical for the simulations, modeling the lung as a quasi-static poroelastic material with a 3-parameter hyperelastic Yeoh model for the solid phase and Darcy's Law for the fluid phase. The material properties are listed in Table 1.

2.2. Pneumothorax: loads and boundary conditions

In normal breathing conditions, the intrapleural pressure is approximately of -500 Pa at the end-of-exhalation. A rupture of the thoracic cavity causes a pneumothorax, establishing an air-pressure gradient at the rupture site resulting in the entrance of air in the thoracic cavity. The pleural pressure increases until reaching atmospheric pressure (0 Pa), and the lung deflates under its own weight.

On the one hand, in the absence of the stress-free configuration, the pneumothorax may be simulated using a functional approach (Alvarez et al. 2021). Instead of a negative pressure at the surface that disappears, a positive pressure of 500 Pa (approximating the change of intrapleural pressure from -500 Pa to zero atmospheric pressure) may be used, in addition to gravity loading to account for the directional movement of the lung.

On the other hand, the stress-free configuration of the lung may be estimated first. In this case, this stress-free configuration is loaded with gravity and a surface pressure of -500 Pa that is subsequently removed to simulate pneumothorax.

2.2. Estimation of stress-free configuration

The stress-free configuration was estimated using an iterative correction procedure (Mira et al. 2018). Given the initial FE mesh extracted from the CT configuration, the objective is to find a new configuration such that after applying the loads of gravity, external pressure, and contacts with the thoracic wall, its equilibrium state is as close as possible to initial CT configuration.

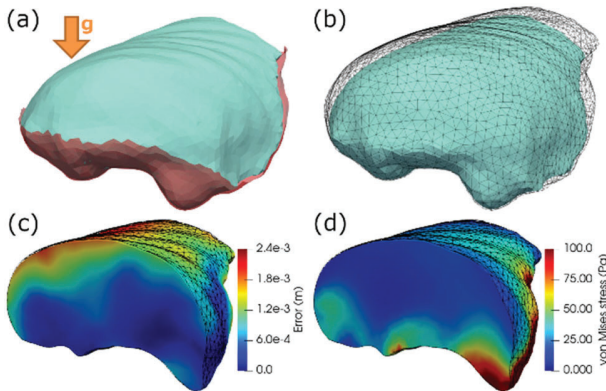


Figure 1. Estimated stress-free configuration after initialization (a) and at the final iteration (b); and spatial distribution of node-to-node error (c) and von Mises Stress (d) after loading with gravity and external pressure. Axial cuts are used in (c) and (d) to show internal information. The black wireframe mesh in (a), (b), and (c) indicates the initial CT geometry.

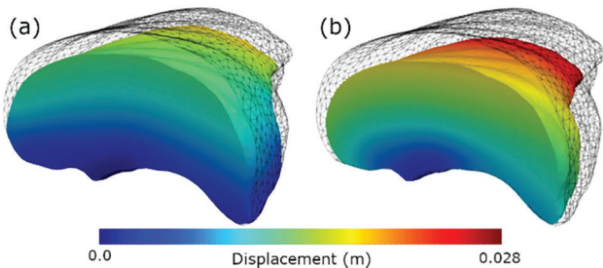


Figure 2. Axial cuts of simulated pneumothorax deformation with the pre-stress (a) and functional (b) approaches. The black wireframe mesh indicates the initial CT geometry.

The initialization of this iterative process requires the application of inverse loads, i.e. a gravity load in the opposite direction and a positive surface pressure. To avoid unrealistic deformation when applying the inverse gravity load, the lung was forced to remain in contact with the mediastinal face of the thoracic wall (red surface in Figure 1(a)). This no-separation contact condition was removed for the iterative process computing the stress-free configuration.

The error at each iteration was quantified by the node-to-node distance between deformed configuration after applying loads and the initial CT configuration. The iterative process was stopped when the change in average node-to-node error was below 0.1 mm.

3. Results and discussion

3.1. Stress-free reference configuration

The application of inverse loading conditions for the initialization procedure provided a first estimation of the stress-free configuration (Figure 1(a)). The iterative procedure improved the estimation of this stress-

free configuration, going from an average node-to-node error of 2.5 mm after initialization, to 0.9 mm at the final iteration (Figure 1(c)). This final estimation error was lower near contact regions, since lung deformation is constrained by contact surfaces, which were generated from the initial CT configuration.

The loading process resulted in a heterogeneous distribution of internal pre-stress (Figure 1(d)), with larger stresses near the mediastinum region, at the contact interface, but overall nonzero everywhere.

3.2. Effects of pre-stress

The resulting deformation after simulating pneumothorax with the functional and pre-stress approaches are illustrated in Figure 2. The average (standard deviation) displacement was of 9.1 mm (\pm 4.0 mm) and of 13.0 mm (\pm 5.4 mm) for the simulations with and without pre-stress, respectively. This larger deformation in the functional approach was statistically significant ($p < .001$, paired t test), and illustrates the important role of internal pre-stress in resisting to deformation. In addition, the total volume loss after pneumothorax was of 23.7% and of 32.5%, respectively. This is, almost 10% more volume loss for the functional simulation approach. Finally, the difference in maximal displacement is over 10 mm, more than an acceptable accuracy for clinical use.

4. Conclusions

This paper takes into consideration the effects of pre-stress for simulating lung pneumothorax. Larger displacement and volume changes were observed when pre-stress was not taken into account, both statistically significant. In the literature, lung pneumothorax is typically simulated using a functional approach, disregarding the effects of pre-stress. Although it is yet unclear which simulation approach should be favored, accounting for pre-stress appears at minimum more realistic. We plan in comparing the two approaches against clinical data in future work.

Disclosure statement

No potential conflict of interest was reported by the authors.

Funding

This work was supported by the ANR framework Images et modèles pour le guidage d'intervention par vidéo-thoroscopie - VATSop (ANR-20-CE19-0015).

References

- Alvarez P, Rouzé S, Miga MI, Payan Y, Dillenseger J-L, Chabanas M. 2021. A hybrid, image-based and biomechanics-based registration approach to markerless intraoperative nodule localization during video-assisted thoracoscopic surgery. *Med Image Anal.* 69:101983.
- Jafari P, Dempsey S, Hoover DA, Karami E, Gaede S, Sadeghi-Naini A, Lee TY, Samani A. 2021. In-vivo lung biomechanical modeling for effective tumor motion tracking in external beam radiation therapy. *Comput Biol Med.* 130:104231.

- Mira A, Carton A-K, Muller S, Payan Y. 2018. A biomechanical breast model evaluated with respect to MRI data collected in three different positions. *Clin Biomech.* 60: 191–199.
- Payan Y, editor. 2012. *Soft tissue biomechanical modeling for computer assisted surgery.* Berlin: Springer.

KEYWORDS Pre-stress; lung; poroelasticity; pneumothorax
 pablo.alvarez@univ-grenoble-alpes.fr